2025 10th International Conference on Technology and Energy Management (ICTEM)

Techno-economic assessment of solar-based Cu-Cl thermochemical hydrogen production plant: A case study

1st Shahin Akbari
Mechanical Engineering
Sharif University of Technology
Tehran, Iran
shahin.akbari@mech.sharif.edu

2nd Mohammad Mahdi Forootan
Energy Engineering
Iran University of Science and Technology
Tehran, Iran
m_furotan@alumni.iust.ac.ir

3rd Maryam Ravangard
Energy Engineering
Sharif University of Technology
Tehran, Iran
ravangard.maryam@energy.sharif.edu

4th Mohammad Ali Bijarchi
Mechanical Engineering
Sharif University of Technology
Tehran, Iran
bijarchi@sharif.edu

2025 10th International Conference on Technology and Energy Management (ICTEM) | 979-8-3315-3862-0/25/$31.00 ©2025 IEEE | DOI: 10.1109/ICTEM66196.2025.11063499

***Abstract*—As the global energy sector undergoes a transition towards decarbonization, Power-to-X technologies play a pivotal role in converting renewable electricity into usable fuels and chemicals. This study examines the technical and economic feasibility of a solar-powered hydrogen production system that is founded on the copper-chlorine (Cu-Cl) thermochemical cycle. A novel configuration is proposed, utilizing carbon dioxide as a heat transfer fluid (HTF) and integrating a heat recovery network to enhance efficiency. In contrast to numerous prior studies that depend on static models, this research employs dynamic, hourly simulations over an entire year, grounded in actual solar data, to evaluate performance under realistic conditions. The results indicate that this system is capable of achieving lower hydrogen production costs in comparison to traditional electrolysis, primarily due to a reduction in electricity consumption. Furthermore, any surplus electricity generated may be sold to the grid, thereby enhancing economic returns. Through multi-objective optimization, the optimal direct normal irradiance (DNI) for the solar input is identified as 881 W/m², resulting in a hydrogen cost of about $5.5 per kilogram.**

Keywords— Cu-Cl Thermochemical cycle; Green hydrogen production; Dynamic simulation; Techno-economic assessment

I. Introduction

One promising strategy for dealing with the fluctuating output of wind and solar power involves the use of Power-to-X technologies, which convert excess electricity into storable energy forms [1]. By transforming surplus electricity generated during peak production into alternative energy carriers, such as hydrogen, PtX enables energy storage for use during periods of high demand or reduced renewable output. By allowing greater adaptability, these systems support grid stability, improve energy system reliability, and ease the incorporation of renewables into large-scale energy infrastructures [1].

Hydrogen holds significant promise as a renewable energy carrier due to its versatility and potential for clean production using solar or wind power [2]. When generated through renewable energy-driven electrolysis, hydrogen serves as an environmentally friendly and sustainable energy storage solution. Green hydrogen can be obtained through multiple renewable energy processes without carbon emissions, making it a key component in the transition to cleaner energy systems.

Electrolysis is the primary technique for producing hydrogen, where water is separated into hydrogen and oxygen through the use of electricity sourced from renewable energy, such as wind or solar power [3]. However, the process is energy-intensive, with high electricity consumption being a major drawback that increases costs and reduces efficiency, mainly when relying on renewables.

The literature proposes various strategies to mitigate electrolysis's energy demands. Approaches such as using high-efficiency electrolyzers with advanced catalytic materials, adopting high-temperature electrolysis to capitalize on thermal energy, and coupling electrolysis with excess renewable power have been explored to lower costs. Nevertheless, achieving a fully cost-effective and scalable solution remains an ongoing challenge.

The Cu-Cl thermochemical cycle stands out as a leading candidate for sustainable hydrogen production. Requiring moderate operating temperatures in the range of 450–530 °C, it is well-suited for integration with thermal inputs from sources like concentrated solar power (CSP) and excess thermal energy from industrial processes. Through a series of thermochemical reactions involving copper and chlorine, the Cu-Cl cycle splits water into hydrogen and oxygen. Unlike traditional electrolysis, it requires significantly less electricity since heat serves as the primary energy input. When combined with advanced heat recovery systems, the cycle achieves high theoretical efficiencies, making it a highly efficient option for hydrogen production.

CSP systems can provide the thermal energy needed to drive the endothermic processes in the cycle. Earlier research often used molten salt as the heat transfer fluid (HTF) to generate steam, which was then used to supply heat to the reactors. However, the copper oxychloride decomposition stage requires temperatures above 500 °C, leaving only a narrow thermal margin between the steam and reactor temperatures, thus limiting heat transfer efficiency. This limitation necessitates high flow rates of molten salt to meet the reactor's heat demands, thereby reducing hydrogen production efficiency. This research introduces a solar-driven configuration that utilizes carbon dioxide as the HTF, complemented by a network of heat exchangers designed to recover and reuse waste heat efficiently.

979-8-3315-3862-0/25/$31.00 ©2025 IEEE

Authorized licensed use limited to: University of Pittsburgh. Downloaded on July 09,2026 at 01:41:23 UTC from IEEE Xplore. Restrictions apply.

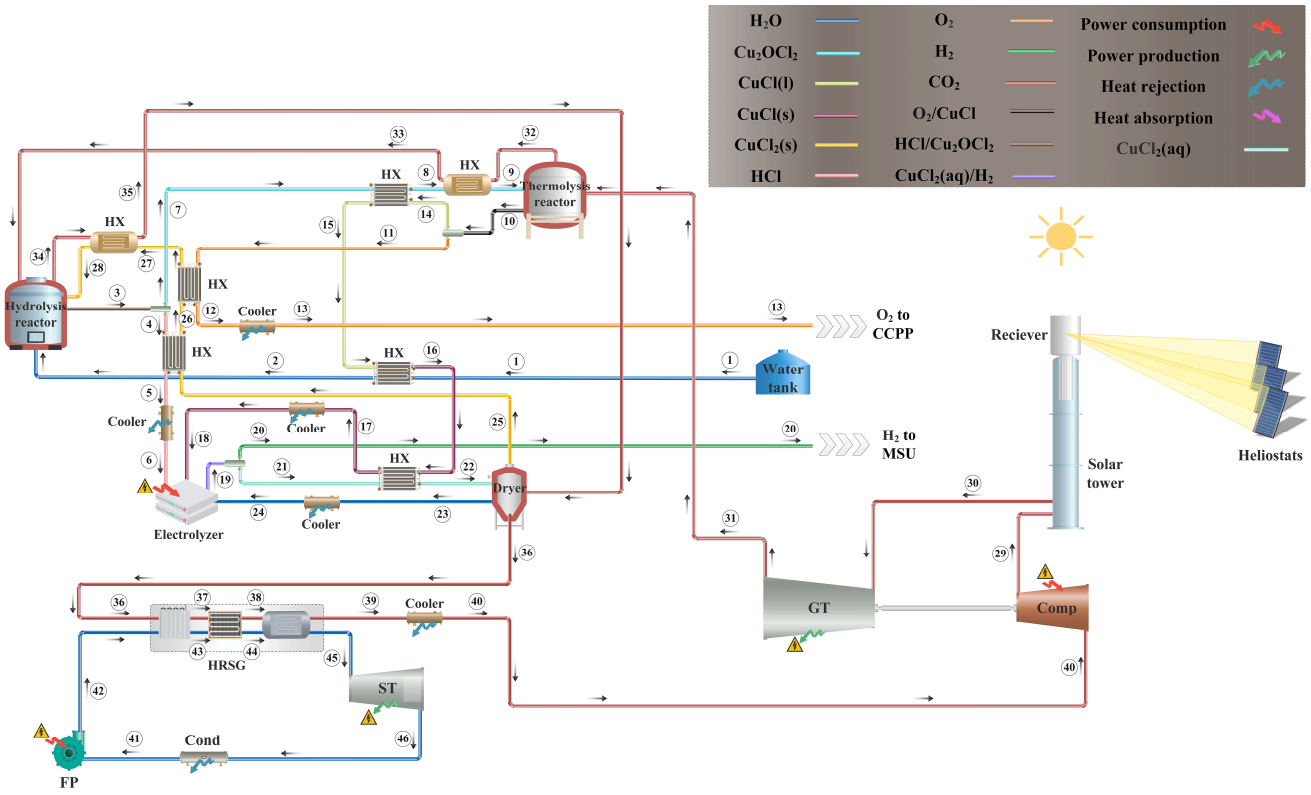

Fig. 1. Schematic of the solar-assisted Cu-Cl cycle for hydrogen generation.

A. *From an Iranian perspective*

Iran's geographic advantages, sunny climate, and ample available land make it a leading candidate for large-scale solar energy development. Its consistently high solar exposure and long daylight hours year-round further strengthen its potential in the region, offering an ideal environment for efficient and reliable solar power generation. The country's extensive desert and semi-desert regions provide vast, underutilized spaces well-suited for the establishment of solar farms, with minimal impact on existing agricultural or urban areas. By strategically investing in solar infrastructure, Iran could not only diversify its energy portfolio and reduce dependence on fossil fuels but also stimulate economic growth through job creation and technological innovation. Moreover, embracing solar energy positions Iran to play a crucial role in regional and global efforts to combat climate change and transition toward a more sustainable energy future.

B. *Motivation and objectives*

The Cu-Cl thermochemical cycle offers a promising candidate for producing green hydrogen by splitting water into hydrogen and oxygen using solar thermal energy and electricity. Although this process requires some electricity, its consumption is significantly lower than conventional electrolysis, resulting in improved energy efficiency. Among its main benefits are enhanced energy performance and strong potential for deployment in large-scale hydrogen production systems. The system is developed and modeled, followed by annual dynamic simulations to assess the proposed hydrogen production system's performance. These simulations account for seasonal fluctuations in solar resource supply and plant operating conditions, comprehensively evaluating system efficiency and performance.

II. System Description

Fig. 1 illustrates a solar-powered Cu-Cl thermochemical cycle devised for hydrogen generation. The process begins with hydrolysis, where water vapor reacts with $CuCl_2$ at around 390°C, yielding copper oxychloride Cu_2OCl_2 and HCl via an energy-absorbing reaction. Next, the Cu_2OCl_2 is directed to the thermolysis reactor, where it is heated to about 530°C. In this step, it breaks down into an endothermic reaction to form molten CuCl and O_2. The products from the previous stages, HCl from hydrolysis and CuCl from thermolysis, are cooled to near room temperature (25°C) before entering the electrolysis unit. There, H_2 is produced, and $CuCl_2$ is regenerated. The regenerated $CuCl_2$ undergoes a drying process, after which it is cycled back to the hydrolysis reactor, enabling the continuous operation of the system.

In contrast to previous configurations, the proposed design combines a combined cycle power plant, operating independently without external power input. Beyond supplying electricity for the electrolysis stage of the Cu-Cl process, the system also produces surplus electricity, which can be exported to the grid for additional economic benefit. Revenue from this electricity sale reduces the overall cost of hydrogen production.

Authorized licensed use limited to: University of Pittsburgh. Downloaded on July 09,2026 at 01:41:23 UTC from IEEE Xplore. Restrictions apply.

III. METHODOLOGY

This study aims to perform an in-depth techno-economic assessment of green hydrogen production potential in Iran. It focuses on analyzing the performance of a solar-integrated Cu-Cl cycle using year-long dynamic simulations. The following section details the modeling approach and methodology applied to evaluate the proposed system's technical and economic viability.

A. Solar power tower modeling

The heat received by the solar tower from the heliostats is calculated by the following relation [4]:

$$\dot{Q}_{rec} = A_h . N_h . DNI . \eta_{opt} \tag{1}$$

where A_h denotes the aperture area of a single heliostat unit, while N_h represents the total number of heliostats in the field. The term *DNI* corresponds to the direct normal irradiance, and η_{opt} signifies the optical efficiency associated with the heliostat mirrors.

The thermal energy lost by the receiver and the amount of heat gained by the HTF are evaluated using the following expressions [5]:

$$\dot{Q}_{loss} = \dot{Q}_{conv} + \dot{Q}_{rad} \tag{2}$$

$$\dot{Q}_{abs} = \dot{Q}_{rec} - \dot{Q}_{loss} \tag{3}$$

For further details, one can see Refs. [5].

B. Cu-Cl cycle modeling

The thermodynamic characteristics of all process streams within the Cu-Cl cycle are evaluated using the Shomate equations [6]. The enthalpy values for each stream are expressed through the following mathematical relationship.

$$h^0 - h^0_{ref} = At + B\frac{t^2}{2} + C\frac{t^3}{3} + D\frac{t^4}{4} - \frac{E}{t} + F - H \tag{4}$$

where,

$$t = \frac{T}{1000} \tag{5}$$

Parameters A-H correspond to the Shomate equation coefficients, sourced from [6].

MATLAB is employed to develop and simulate the full system model. This model incorporates detailed energy balance equations for each component to ensure accurate mass and heat flow interaction calculations. It is also assumed that no heat loss occurs in the thermochemical Cu-Cl cycle.

C. Thermodynamic Efficiency Metrics

In this study, the system is simulated hourly throughout the year. The simulation approach involves segmenting the entire year into hourly time steps and conducting numerical integration for each interval. The proposed system's energy and exergy efficiencies are computed hourly and aggregated to determine the annual performance.

$$\eta_{I,HPU} = \frac{\int_0^{8760}\left(\dot{m}_{H_2}(h).LHV_{H_2} + \dot{W}_{net}(h)\right)dh}{\int_0^{8760}\dot{Q}_{sun}(h)dh} \tag{6}$$

$$\eta_{II,HPU} = \frac{\int_0^{8760}\left(\dot{m}_{H_2}(h).ex^{ch}_{H_2} + \dot{W}_{net}(h)\right)dh}{\int_0^{8760}\dot{E}x_{sun}(h)dh} \tag{7}$$

where $\dot{m}_{MeOH}$, LHV, $\dot{W}_{net}$ is the hydrogen production rate, the lower heating value, and the net power produced from the power plant, respectively.

D. Economic analysis

Table 1 lists the purchased equipment costs (CPE) associated with each system component, which constitute a major portion of the direct capital expenditures (CAPEX). The overall CPE is obtained by summing the individual costs of all equipment units included in the design.

TABLE 1. CAPITAL COST ESTIMATION EQUATIONS FOR KEY SYSTEM COMPONENTS [7, 8].

Component	***CAPEX*** $
Heliostat mirrors	$75 N_h A_h$
Solar receiver	$48500 A_{rec}$
Solar tower	$782320 \exp\left(0.01130 H_{tower}\right)$
Hydrolysis and Thermolysis reactors	$\exp\left[3.4974 - 0.4485 \ln\left(V_R\right) + 0.1074\left(\ln\left(V_R\right)\right)^2\right]$
Drying unit	$\exp\left[4.5097 - 0.8269 \ln\left(V_{dryer}\right) + 0.1344\left(\ln\left(V_{dryer}\right)\right)^2\right]$
Electrolyzer stack	$230 N_{cell} A_{cell}$
Compressor	$\left(\frac{71.1\,\dot{m}}{0.92 - \eta_c}\right)(PR)\,Ln(PR)$
Gas turbine	$\left(\frac{479.34\dot{m}}{0.92 - \eta_{GT}}\right)Ln(PR)\left[1 + \exp\left(0.036 T_{inlet} - 54.4\right)\right]$
Bayonet heat exchangers	$\exp\left[4.2768 - 0.0495 \ln\left(A\right) + 0.1431\left(\ln\left(A\right)\right)^2\right]$
Shell and tube heat exchangers	$\exp\left[4.3247 - 0.3030 \ln\left(A\right) + 0.1634\left(\ln\left(A\right)\right)^2\right]$

Authorized licensed use limited to: University of Pittsburgh. Downloaded on July 09,2026 at 01:41:23 UTC from IEEE Xplore. Restrictions apply.

Component	*CAPEX* $
HRSG	$6570\left[\left(A_{eco}\right)^{0.8}+\left(A_{eva}\right)^{0.8}+\left(A_{sup}\right)^{0.8}\right]+21276\dot{m}_{w}+1184.4\dot{m}_{CO_2}^{1.2}$
Pump	$1120\left(\frac{\dot{W}_{FP-RC}}{1000}\right)^{0.8}$
Steam turbine	$6000\left(\frac{W_{ST}}{1000}\right)^{0.7}$
Condenser	$516\left(A_{cond}\right)^{0.6}$

Additional cost components contributing to the total CAPEX are detailed in [9].

The operating expenditures (OPEX), encompassing costs associated with plant operation and equipment servicing, are described in [10]. The approach from Ref. [2] is applied is used to transform both OPEX and CAPEX into total plant costs, which are then utilized to calculate the hydrogen production cost. The economic data used for this analysis are summarized in Table 2.

TABLE 2. INPUT DATA FOR TECHNO-ECONOMIC EVALUATION.

variables	*Value*
Assumed system lifetime (year)	30
Interval for stack replacement (year)	5
Discount rate	0.08
Electricity cost ($/MW.h)	40

Eq. (8) is used to calculate the levelized cost of hydrogen (LCOH).

$$LCOH = \frac{\left(CAPEX_{annully}+OPEX_{fix}\right)_{total}-revenue_{electricity}}{\int_0^{8760}\dot{m}_{H_2}(h)dh} \quad (8)$$

The revenue generated from electricity sales is determined using the following equation:

$$revenue_{electricity} = LCOE_{grid}\times\frac{\int_0^{8760}\dot{W}_{net}(h)dh}{3600} \quad (9)$$

IV. RESULTS AND DISCUSSION

This section provides a detailed evaluation of the proposed hydrogen production system, analyzing its performance across different operating conditions and design parameters.

A. Meteorological data

Reliable weather data is critical for capturing the system's behavior under realistic environmental conditions. In this work, climate inputs for Sirjan, Iran, were sourced from the Visual Crossing database [11], a reliable historical weather information provider. The dataset includes key parameters such as direct normal irradiance (DNI), ambient temperature, and wind speed for the year 2023. Fig. 2 illustrates the daily variation of DNI along with two specific design cases, which are discussed in detail in the subsequent sections.

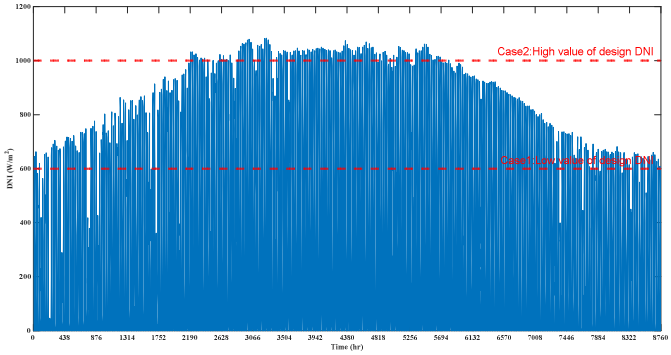

Fig.2. Yearly DNI distribution for 2023 and corresponding design cases.

B. Effect of the design DNI

Establishing a conceptual design is essential before proceeding to the comprehensive system design phase. A critical aspect of this stage is selecting the design DNI, which represents the direct normal irradiance at which the hydrogen production plant operates at its rated capacity. This design DNI is used to size the solar field appropriately, ensuring the system achieves its rated production capacity.

Two design cases are evaluated, as depicted in Fig. 2. Selecting the appropriate design radiation level is crucial to account for daily and seasonal fluctuations in solar radiation, optimizing the plant's performance.

Figure 3 displays the monthly variation of thermal energy captured by the HTF and the corresponding heat losses incurred at the solar receiver for both design scenarios. The analysis reveals that case 2 experiences lower heat absorption, primarily due to the CSP system's lower capacity factor. This outcome is linked to the heliostat field configuration, which is influenced by the chosen design DNI. Specifically, a higher design DNI results in a smaller heliostat field being sufficient to meet the target power output. However, when real-time solar irradiance values fall below the design threshold, the reduced field area captures less solar energy, thereby decreasing the overall thermal input to the HTF.

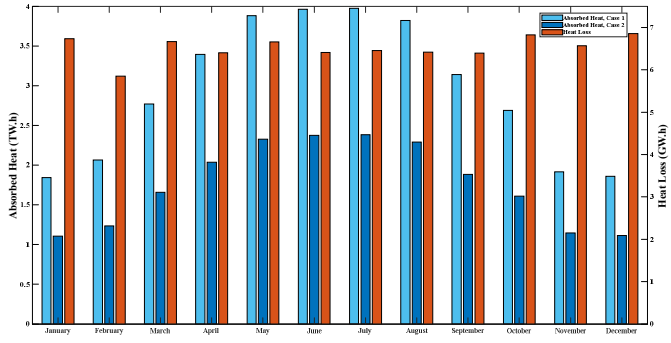

Fig. 3. Monthly performance of heat absorption and loss.

Authorized licensed use limited to: University of Pittsburgh. Downloaded on July 09,2026 at 01:41:23 UTC from IEEE Xplore. Restrictions apply.

Fig. 4 compares the monthly average hydrogen production between the two cases. The data reveals that hydrogen production in both cases falls short of the ideal benchmark, representing the optimal production target. The primary cause of this discrepancy is the limited operating hours of the CSP system, constrained by the solar energy supply. Hydrogen production is closely linked to solar radiation and, as such, cannot be maintained continuously.

Additionally, the CSP system's capacity factor, defined as the ratio of realized energy production to its theoretical maximum, remains below unity, indicating that the system does not consistently operate at full capacity. Similarly, the utilization ratio, reflecting the fraction of time the plant is actively producing hydrogen relative to total available hours, also falls short of one. Both metrics vary seasonally due to fluctuations in solar irradiance, leading to notable variations in the plant's operational efficiency throughout the year. Fig. 5 shows these monthly variations, further explaining the lower-than-expected hydrogen production.

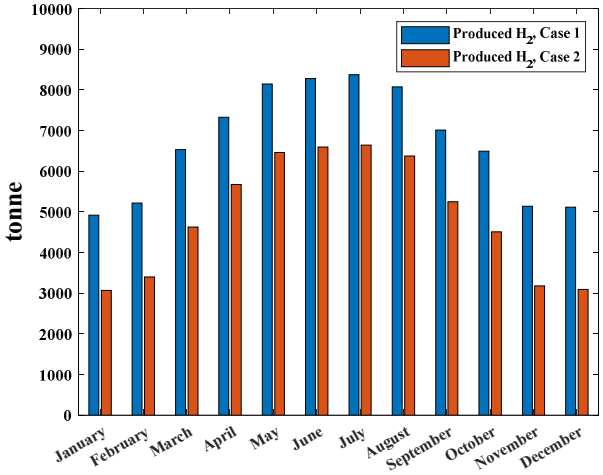

Fig. 4. Monthly variation of hydrogen production for cases 1 and 2.

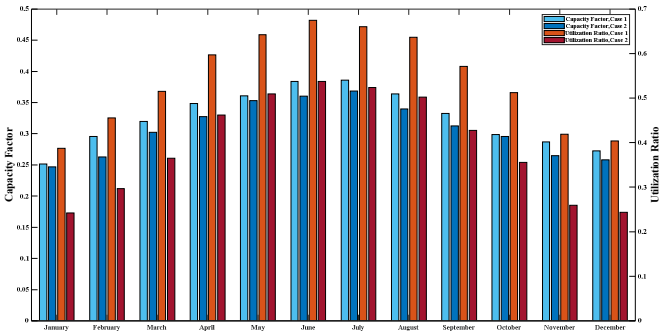

Fig. 5. Variation in Capacity Utilization and Hydrogen Production Across Months.

Figure 4 illustrates that hydrogen production in case 1 consistently exceeds that of case 2 throughout the year. This discrepancy is primarily due to the larger heliostat field in case 1, which enables greater solar energy capture and, consequently, higher thermal power output. The increased solar input allows the CSP plant to operate for more hours, enhancing the utilization ratio. As a result, case 1 achieves both extended operational periods and higher hydrogen yields than case 2.

While case 1 yields greater hydrogen output, it is accompanied by a certain limitation. The larger heliostat field may cause periods of excess solar energy during peak irradiance, which the CSP system cannot fully absorb or utilize due to design constraints. This mismatch reduces overall system efficiency, as surplus energy is effectively wasted. Since the CAPEX of the CSP plant is fixed annually, the inability to fully utilize available solar energy during periods of high irradiance results in elevated hydrogen generation costs and a less favorable return on investment.

The dynamic simulation for 2023 is conducted to analyze the cost distribution of each subsystem involved in hydrogen production for both cases. As illustrated in Figures 6 and 7, solar field expenditures constitute the largest share of total costs in both scenarios. In case 1, the hydrogen generation plant represents approximately 60% of the total capital investment, compared to 53% in case 2. Notably, the solar field cost is substantially greater in case 1 due to the larger number of heliostat mirrors needed. This expanded heliostat field increases solar energy capture, boosting hydrogen output but also significantly raising the capital investment associated with the solar subsystem.

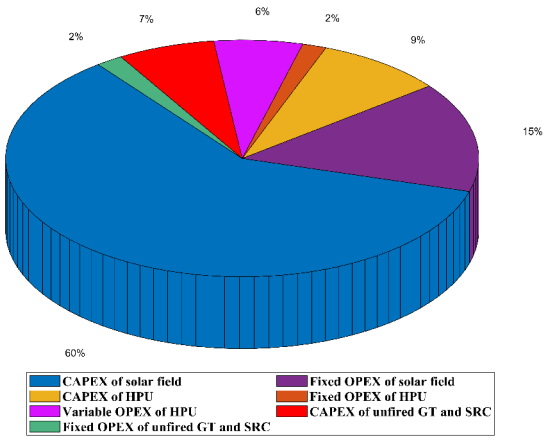

Fig. 6. Detailed cost structure of hydrogen production for case 1.

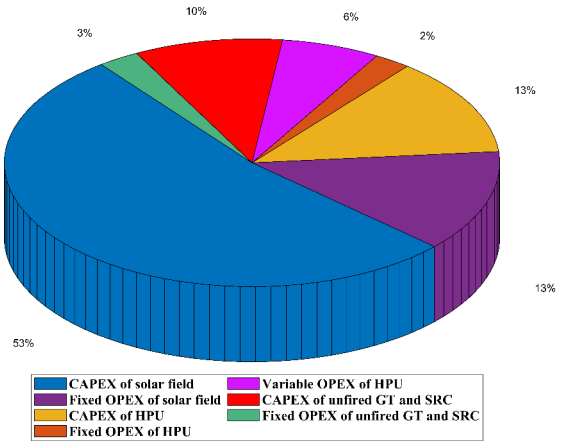

Fig. 7. Detailed cost structure of hydrogen production for case 2.

Authorized licensed use limited to: University of Pittsburgh. Downloaded on July 09,2026 at 01:41:23 UTC from IEEE Xplore. Restrictions apply.

In case 1, the heliostat field represents the most significant cost driver in hydrogen generation, owing to the extensive heliostat array. In contrast, case 2 incurs lower solar field costs due to a smaller heliostat configuration. This highlights the trade-off in case 1 between enhanced hydrogen output and the higher capital investment required for solar energy collection.

C. *Trade-off between cost and efficiency*

This section applies a multi-objective optimization framework to identify the most suitable value for design DNI in the CSP system. The approach simultaneously addresses two fundamental goals: enhancing exergy efficiency and reducing the LCOH, both essential to ensuring technical and economic viability. A genetic algorithm is employed to tackle the optimization problem, resulting in a Pareto front of non-dominated solutions. The LINMAP decision-making method is then used to select the most balanced solution from the trade-off curve.

TABLE 3. SIMULATION OUTCOMES FOR THE PROPOSED HYDROGEN PRODUCTION PLANT POWERED BY SOLAR THERMAL ENERGY.

Parameters	***Case 1: Design DNI=600***	***Case 2: Design DNI=1000***	***Optimal design DNI= 881***
Energy efficiency (%)	21.3	26	25.4
Exergy efficiency (%)	23.5	28.6	27.9
LCOH ($/kg)	6.4	5.7	5.5
Hydrogen output (tonne/year)	80,624	58,874	65,314
Oxygen output (tonne/year)	480,340	350,760	389,120
Yearly power generation (GW.h)	9,500	6,900	7,700
Total heliostat numbers	201,949	121,170	137,573
Capacity factor (%)	38.6	28	31
Utilization Rate (%)	45.5	43	43.8

V. CONCLUSION

Through dynamic simulations of the system's year-round operation and optimization of the design DNI, the proposed solar-driven thermochemical system in the optimized scenario achieves enhanced energy efficiency and cost reduction. The results demonstrate that a solar-based thermochemical plant offers a cost-effective solution for PtX applications, supporting the broader utilization of renewable energy. Key findings include:

- The annual performance of the CSP plant is significantly influenced by the balance between the selected design DNI and the scale of the heliostat field. In case 1, a larger heliostat field captures more solar energy under diverse conditions but may result in unutilized energy during periods of high radiation. A smaller heliostat field reduces the capacity factor in case 2. An optimum DNI value for the development of the CSP system is identified. Under these conditions, the LCOH is $5.5/kg in the optimized case, representing a 14.1% reduction compared to case 1 and a 3.5% decrease relative to case 2.
- One of the primary advantages of the proposed solar-driven hydrogen production system is its self-sufficiency, operating without reliance on external energy sources. Moreover, the system produces surplus power that can be exported to the grid, creating an additional revenue stream that helps offset hydrogen production costs and improves overall economic performance.
- The techno-economic analysis underscores a significant benefit of the solar-driven thermochemical hydrogen generation approach: substantially reduced electricity consumption compared to traditional electrolyzer-based methods. Unlike conventional methods, where variable operating expenses constitute a major portion of the costs, the proposed system's cost structure is dominated by capital expenditures, minimizing the impact of operating expenses.

REFERENCES

[1] G. Buffo, P. Marocco, D. Ferrero, A. Lanzini, and M. Santarelli, "Power-to-X and power-to-power routes," in *Solar hydrogen production*: Elsevier, 2019, pp. 529-557.

[2] H. Nami, O. B. Rizvandi, C. Chatzichristodoulou, P. V. Hendriksen, and H. L. Frandsen, "Techno-economic analysis of current and emerging electrolysis technologies for green hydrogen production," *Energy Conversion and Management,* vol. 269, p. 116162, 2022.

[3] G. Chisholm, T. Zhao, and L. Cronin, "Hydrogen from water electrolysis," in *Storing Energy*: Elsevier, 2022, pp. 559-591.

[4] M. E. Demir and I. Dincer, "Development of a hybrid solar thermal system with TEG and PEM electrolyzer for hydrogen and power production," *International Journal of Hydrogen Energy,* vol. 42, no. 51, pp. 30044-30056, 2017.

[5] J. Kim, J.-S. Kim, and W. Stein, "Simplified heat loss model for central tower solar receiver," *Solar Energy,* vol. 116, pp. 314-322, 2015.

[6] *National Institute of Standards and Technology (NIST)*. Available: https://webbook.nist.gov/chemistry/form-ser/

[7] A. Z. Ozbilen, "Development, analysis and life cycle assessment of integrated systems for hydrogen production based on the copper-chlorine (Cu-Cl) cycle," 2013.

[8] S. Akbari, A. Hakkaki-Fard, and M. B. Shafii, "Feasibility assessment of power-to-methanol through solar thermochemical hydrogen production plant: A case study," *Energy Conversion and Management,* vol. 333, p. 119787, 2025.

[9] A. Bejan, G. Tsatsaronis, and M. J. Moran, *Thermal design and optimization*. John Wiley & Sons, 1995.

[10] R. Turton, R. C. Bailie, W. B. Whiting, and J. A. Shaeiwitz, *Analysis, synthesis and design of chemical processes*. Pearson Education, 2008.

[11] Weather Data Services | Visual Crossing [Online]. Available: https://www.visualcrossing.com/weather/weather-data-services

Authorized licensed use limited to: University of Pittsburgh. Downloaded on July 09,2026 at 01:41:23 UTC from IEEE Xplore. Restrictions apply.